American Mineralogist, Volume 77, pages 904–910, 1992

An atomic force microscope (AFM) study of the calcite cleavage plane: Image averaging in Fourier space

ALAN L. RACHLIN, GRANT S. HENDERSON
Department of Geology, University of Toronto, Toronto, Ontario M5S 3B1, Canada
M. CYNTHIA GOH
Department of Chemistry, University of Toronto, Toronto, Ontario M5S 1A1, Canada

ABSTRACT

The cleavage plane of calcite (in equilibrium with H_2O) has been examined at nearly atomic resolution using an atomic force microscope (AFM). The images obtained suggest that there is minimal reconstruction of the surface. The cleavage plane exhibits a rectangular unit cell 0.74(5) nm by 0.48(2) nm, which is in general agreement with both the unit cell calculated from the bulk structure and that derived from low-energy electron diffraction (LEED) images. Individual AFM images were too noisy to resolve atoms, and the surface pattern appeared to vary. Conversion of the images into Fourier space showed a consistent pattern of periodicities similar to that observed in previously published LEED images, but the individual peak locations and intensities varied slightly from image to image. For periodic surfaces, averaging of images in Fourier space improves image quality without loss of information.

INTRODUCTION

Calcite is one of the most ubiquitous materials at the Earth's surface. It occurs in geological settings as diverse as near shore marine muds and carbonatites (Reeder, 1983). However, although it is a simple salt and has been studied extensively, the geochemistry of calcite is complex and remains imperfectly understood.

Many studies have examined the bulk interaction between calcite and various aqueous impurities (cf. Kitano et al., 1975, 1979a, 1979b; Reddy and Wang, 1980; Söhnel and Mullin, 1982; Mucci and Morse, 1983). More recently, interactions at the mineral's surface have been studied using X-ray photoelectron spectroscopy (XPS), Auger electron spectroscopy (AES), or low-energy electron diffraction (LEED) (cf. Bancroft et al., 1977a, 1977b, 1979; Brown, 1978; Mucci et al., 1985; Mucci and Morse, 1985; Fulghum et al., 1988; Zachara et al., 1989; Stipp and Hochella, 1991). However, these methods are technically demanding, as they require that the sample be under vacuum.

The atomic force microscope (AFM) was developed in 1985 (Binnig et al., 1986) as an extension of scanning tunneling microscope (STM) technology. Samples can be imaged under ambient conditions, in contact with solutions or in a vacuum. Sample preparation is relatively simple, and the AFM can be used to image both conducting and nonconducting materials. AFM technology is still young and has only recently been applied to earth science problems. It has been used to image muscovite (Drake et al., 1989), illite and montmorillonite (Hartman et al., 1990), clinoptilolite (Weisenhorn et al., 1990), hematite (Johnsson et al., 1991), graphite (Binnig et al., 1986), sodium chloride (Meyer and Amer, 1990), albite (Drake and Hellmann, 1991), and lizardite (Wicks et al., 1992).

To date, atomic resolution AFM images have been difficult to obtain because the images could not be reproduced. This study attempts to characterize the unit cell of the calcite cleavage plane by performing a statistical analysis of the periodicities exhibited by multiple AFM images in Fourier space.

CALCITE STRUCTURE

Calcite ($CaCO_3$) is hexagonal, space group $R\bar{3}c$, with hexagonal unit-cell parameters $a = 0.4990$ nm, $c = 1.700$ nm, $Z = 6$, as determined by X-ray diffraction (Chessin et al., 1965). As seen from Figure 1, the structure consists of alternating layers of Ca^{2+} and CO_3^{2-} groups oriented perpendicular to the c axis, with interionic bonding between layers. Carbonate groups within a layer are all coplanar and have identical orientations, and alternate layers are rotated 180° with respect to the layers above and below. Calcite has perfect rhombohedral cleavage $\{10\bar{1}4\}$, which intersects the alternating layers at 44°37′. If the conformation of a cleavage surface is consistent with the mineral's bulk structure, then it should consist of alternating rows of Ca^{2+} and CO_3^{2-}. The carbonate groups should all be inclined with respect to the plane such that one O atom lies above it, one in it, and one below it.

EXPERIMENTAL

Images were obtained using a Digital Instruments Inc. Nanoscope II AFM equipped with a standard A head. This equipment has been previously described by Hoch-

0003–004X/92/0910–0904$02.00

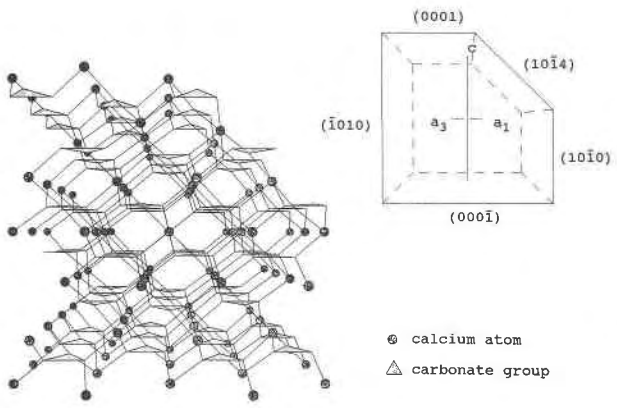

Fig. 1. Calcite structure, projection parallel to [1$\bar{2}$10].

ella et al. (1990). A Si_3N_4 wide-legged 100-μm triangular cantilever was used throughout this study. Colorless and transparent material ("iceland spar") from an unknown locality was cleaved into plates approximately 2 mm thick. A fluid cell was filled with Aldrich HPLC H_2O (glass distilled and filtered through 0.5-μm filters) and was allowed to equilibrate for at least 2 h. Because the cantilever is triangular and contacts the surface to be scanned at an angle, its mechanical properties vary depending on the scan direction. In addition, if the cleavage plane contains inclined CO_3 groups, then the orientation of the sample with respect to the tip may also affect image quality. For this study the cleavage plate was placed in the microscope head in three different orientations. Orientation 1 was such that the projection of the positive **c** axis onto the cleavage plane (**c**′) was approximately parallel to the positive scan direction of the y-piezo. Orientation 2 placed the projection parallel to negative x-piezo scan direction, and orientation 3 placed it parallel to the positive x-piezo scan direction.

Results and discussion

When the cleavage surface was examined in equilibrium with H_2O, periodic structures were observed, but their shape appeared to vary from image to image. The signal to noise ratio remained poor. No atomic or molecular scale resolution was obtained when the sample was equilibrated for less than 1½ h, presumably because calcite was still dissolving. Equilibration for as long as 72 h resulted in no discernible change in image quality. Figure 2 is a representative sample of raw images, captured in a variety of orientations. For clarity, they have been rotated so that **c**′ is vertical in each image in the figure.

When the images were transformed into Fourier space using a two-dimensional fast Fourier transform (2DFFT) algorithm, a consistent pattern of periodicities was observed. However, when measured using polar coordinates, the radial (R), angular (θ), and intensity (I) components of each periodicity varied slightly from image to image. This appears to be the reason that different images of the same surface appear to be quite different. Figure 3 shows the 2DFFT image of each of the images in Figure 2. Figure 4 is a schematic illustration of the average observed 2DFFT pattern, based on examination of 119 images. The most frequently observed peaks have been arbitrarily labeled for ease of reference. By measuring R, θ, and I for each of the frequently observed peaks, it becomes possible to calculate mean values and standard deviations for the observed periodicities. Table 1 lists the measured R, θ, and σ of periodicities in Fourier space in the 16 best images obtained from samples in orientations 1 and 3, with various applied rotations. Intensity (I) is omitted to simplify the illustration. The variability in R and θ is caused in part by determinate error arising from the quantization of cursor movement. The quality of images obtained in orientation 2 was consistently poorer than that of the other orientations, and therefore images in that orientation were not used. As set out in Table 1, the cleavage surface in equilibrium with H_2O exhibits a rectangular unit cell of 0.74(5) nm by 0.48(2) nm. This is in general agreement with the calculated unit cell of 0.808 $\pm$ 0.001 nm by 0.4990 $\pm$ 0.0002 nm using the cell parameters of Chessin et al. (1965).

Table 1. Measured R (nm), θ (°), and σ of periodicities in Fourier space in the 16 best images obtained in this study

Peak	No. obs.	R_{mean}	θ_{mean}	σ_R	σ_θ
a	16	0.48	180.39	0.02	2.44
b	15	0.40	148.59	0.02	2.31
c	13	0.74	93.28	0.05	4.68
d	16	0.41	34.33	0.02	1.47
e	9	0.29	130.31	0.02	2.28
f	14	0.36	92.28	0.02	4.92
g	7	0.30	57.87	0.01	4.58
h	2	0.24	181.46	0.00	4.21
n	5	0.25	97.27	0.02	3.55
p	4	0.18	49.05	0.01	3.97

Figure 5a shows the best unfiltered image of the calcite cleavage plane obtained in this study. In Figure 5b the image has been filtered using the 2DFFT algorithm to retain all observed periodic maxima in Fourier space (13 unique peaks). In both Figures 5a and 5b the alternating rows of Ca^{2+} and CO_3^{2-} can be clearly seen. Finally, in Figure 5c we have applied a hard filter consisting of three lowpass filters, an algorithm to eliminate image bow, and a 2DFFT filter to remove noise. The essential features of the original image can still be resolved. A projection of the cleavage plane was drawn using fractional atomic coordinates from Chessin et al. (1965) and the observed unit cell; it has been superimposed on Figures 5b and 5c. Ionic radii have been reduced to make the structure easier to visualize. There is a good correlation between the observed image and the projection; indeed, it appears that the carbonate O that projects out of the plane is somewhat better visualized than the O that should, in theory, lie in the crystal.

The Fourier transform of a crystalline surface should be the same as the LEED image of that surface. The LEED image of the calcite cleavage plane cleaved in air and after dissolution in H_2O has recently been examined by Stipp

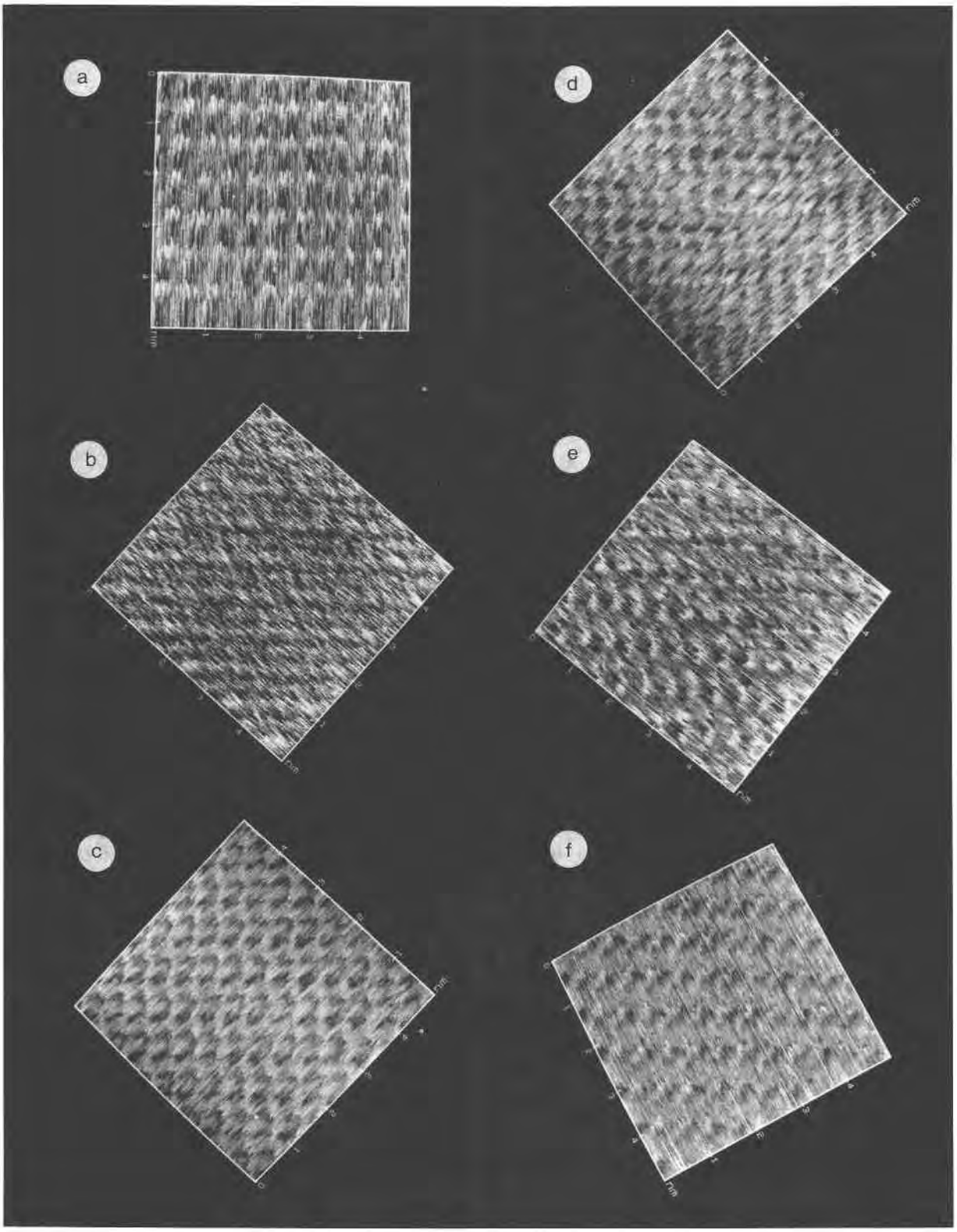

Fig. 2. Unfiltered images of the calcite cleavage plane: (**a**) orientation 3 rotated 180°, (**b**) orientation 3 rotated 135°, (**c**) orientation 1 rotated 135°, (**d**) orientation 1 rotated 135°, (**e**) orientation 1 rotated 30°, (**f**) orientation 1 rotated 60°.

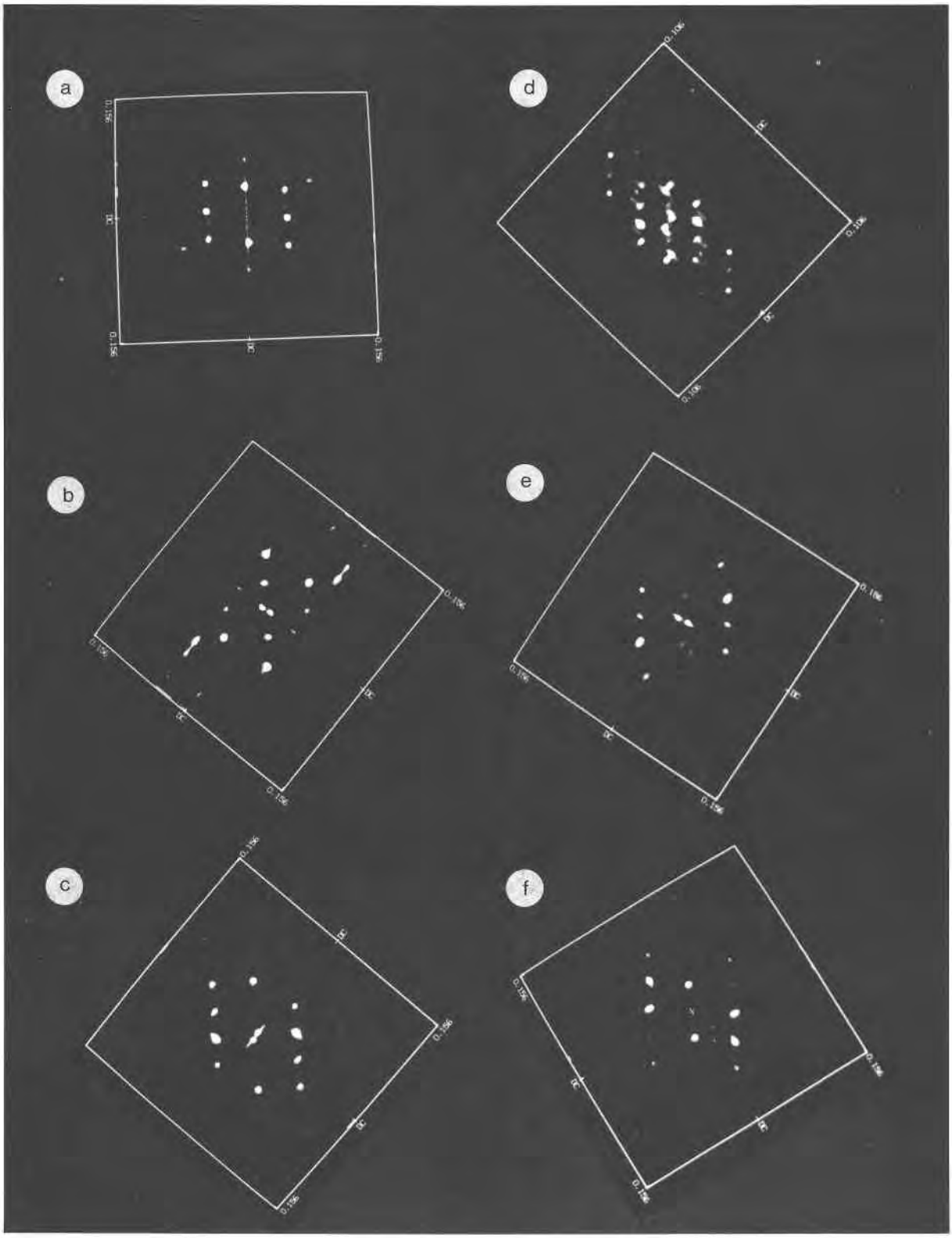

Fig. 3. The 2DFFT images of images in Figure 2a–2f.

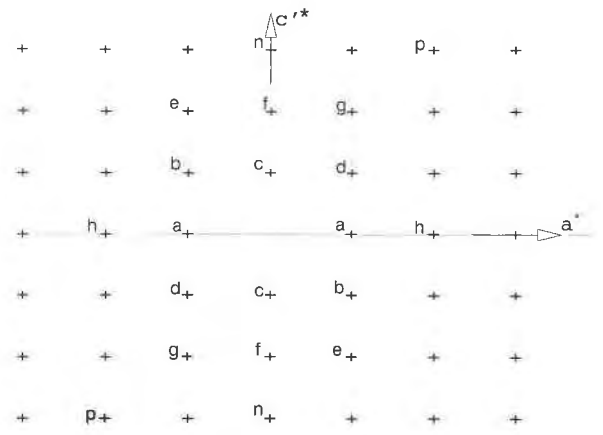

Fig. 4. Schematic illustration of the average observed 2DFFT image of the calcite cleavage plane, based on 119 images. The most frequently observed peaks have been arbitrarily labeled for ease of reference.

and Hochella (1991). They report a rectangular unit cell of dimensions 0.811(25) by 0.497(14) nm for material cleaved in air and 0.816(23) by 0.505(14) nm after dissolution, in general agreement with the results reported here. Stipp and Hochella (1991) also report diffuse extra reflections that effectively double the periodicity in the ≈0.5 nm direction, and they suggest that these additional reflections may represent slightly different orientations of some surface CO_3 groups. Analogous peaks are not observed in this study. If the additional observed reflections were caused by the CO_3 groups, that would imply that the CO_3 groups along the rows take two different but alternating orientations with respect to the cleavage plane. We suggest that a more plausible explanation of these reflections is simply small domains of ordering of cationic impurities as described by Reksten (1990).

Friedbacher et al. (1991) report having imaged the {0001} plane of commercially available powdered calcite and of biogenic calcite from the sea urchin *Strongylocentrotus purpuratus* at atomic resolution. In view of calcite's perfect rhombohedral cleavage and, more importantly, the relative rarity of {0001}, we suspect that the reported images are in fact of the cleavage $\{10\bar{1}4\}$ and not {0001}. The images presented by Friedbacher et al. (1991) are generally similar to the images observed in this study. Examination of the 2DFFT image's peak pattern should resolve the identity of the plane imaged.

Examination of Figure 4 and Table 1 suggests that σ for R and θ are proportionally larger for those peaks lying along **c**′ in Fourier space (**c**′*) (c, f, and n in Fig. 4). This corresponds to the periodicity between the alternating rows of Ca and CO_3 if the cleavage surface is represented by a section through the bulk structure. The general

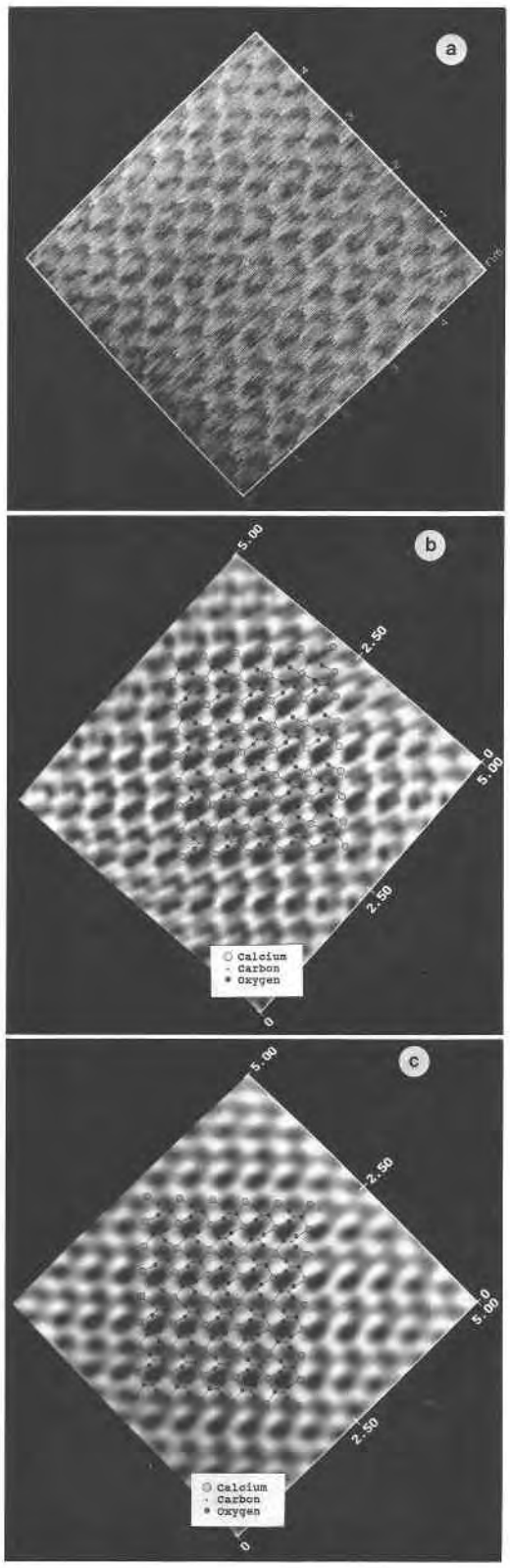

Fig. 5. Best image obtained of the calcite cleavage plane. (**a**) Unfiltered image, (**b**) filtered using 2DFFT algorithm to retain all observed periodic maxima (13 unique peaks), (**c**) hard filter using three lowpass filters, an algorithm to eliminate image bow, and a 2DFFT filter to remove noise.

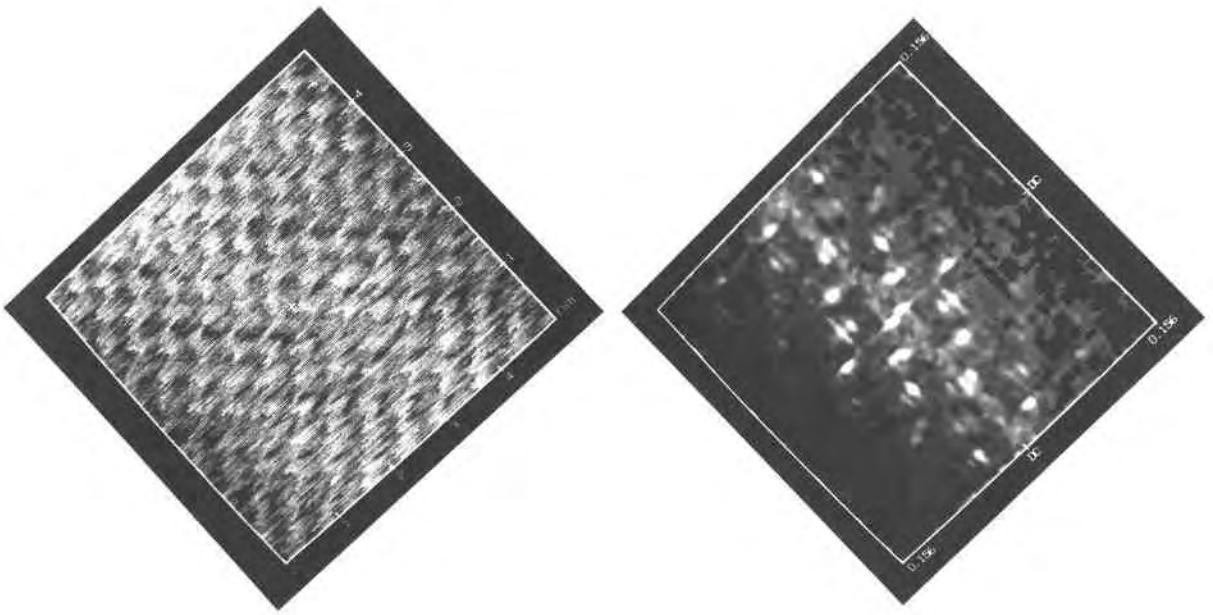

Fig. 6. A 2DFFT image showing splitting of every other peak. We suggest that this may be caused by a slightly misaligned superstructure of some sort.

agreement between the calculated and observed unit cells confirms that the cleavage plane is similar to a section through the bulk structure and that little reconstruction takes place. We suggest that the larger σ for periodicities along c'* may be caused by slight random variation in the inclination of the carbonate groups with respect to the surface.

Finally, some of the images obtained during this study showed consistent periodic splitting of peaks in Fourier space as shown in Figure 6. Because not every peak is split, we believe that the splitting is not caused by twinning or some sort of dislocation. This splitting is difficult to interpret. By analogy to single-crystal X-ray crystallographic relations, it appears to imply a slightly misaligned superstructure of some sort.

Summary and conclusion

In this study the AFM has been used to obtain near atomic resolution of the surface of the calcite cleavage plane in equilibrium with H_2O. The observed surface pattern is variable, but examination of the images in Fourier space discloses a consistent pattern of periodicities, with slight variations in the R and θ of the peaks from image to image. Measurement of R and θ for peaks in Fourier space of multiple images allows a mean observed rectangular unit cell of 0.74(5) by 0.48(2) nm to be derived. Filtering by means of averaging images in Fourier space may allow unit-cell dimensions to be extracted from otherwise noisy and unusable images of periodic surfaces.

A comparison of AFM and LEED results for the calcite cleavage plane suggests that similar surface information can be obtained with both techniques. For many applications the AFM's relative simplicity of instrumental setup and sample preparation will make it the instrument of choice.

Acknowledgments

The authors thank Digital Instruments for advice on instrumental settings, K. Gorra for photographic assistance, and M.F. Hochella, Jr. for his careful review of an earlier draft. This study was supported by a Natural Sciences and Engineering Research Council of Canada operating grant to G.S.H.

References cited

Bancroft, G.M., Brown, J.R., and Fyfe, W.S. (1977a) Calibration studies for quantitative X-ray photoelectron spectroscopy of ions. Analytical Chemistry, 49, 1044–1048.

——— (1977b) Quantitative X-ray photoelectron spectroscopy (ESCA): Studies of Ba^{2+} sorption on calcite. Chemical Geology, 19, 131–144.

——— (1979) Advances in, and applications of, X-ray photoelectron spectroscopy (ESCA) in mineralogy and geochemistry. Chemical Geology, 25, 227–243.

Binnig, G., Quate, C.F., and Gerber, C. (1986) Atomic force microscope. Physical Review Letters, 56, 930–933.

Brown, J.R. (1978) Adsorption of metal ions by calcite and iron sulfides: A quantitative X-ray photoelectron spectroscopy study. Ph.D. dissertation, University of Western Ontario, London, Ontario, Canada.

Chessin, H., Hamilton, W.C., and Post, B. (1965) Position and thermal parameters of oxygen atoms in calcite. Acta Crystallographica, 18, 689–693.

Drake, B., and Hellmann, R. (1991) Atomic force microscopy imaging of the albite (010) surface. American Mineralogist, 76, 1773–1776.

Drake, B., Prater, C.B., Weisenhorn, A.L., Gould, S.A.C., Allbrecht, T.R., Quate, C.F., Connell, D.S., Hansma, H.G., and Hansma, P.K. (1989) Imaging crystals, polymers, and processes in water with the atomic force microscope. Science, 243, 1586–1589.

Friedbacher, G., Hansma, P.K., Ramli, E., and Stucky, G.D. (1991) Imaging powders with the atomic force microscope: From biominerals to commercial materials. Science, 253, 1261–1263.

Fulghum, J.E., Bryan, S.R., Linton, R.W., Bauer, C.F., and Griffis, D.P. (1988) Discrimination between adsorption and coprecipitation in aquatic

particle standards by surface analysis techniques: Lead distributions in calcium carbonates. Environmental Science and Technology, 22, 463–467.

Hartman, H., Sposito, G., Yang, A., Manne, S., Gould, S.A.C., and Hansma, P.K. (1990) Molecular scale imaging of clay mineral surfaces with the atomic force microscope. Clays and Clay Minerals, 38, 337–342.

Hochella, M.F., Jr., Eggleston, C.M., Elings, V.B., and Thompson, M.S. (1990) Atomic structure and morphology of the albite {010} surface: An atomic-force microscope and electron diffraction study. American Mineralogist, 75, 723–730.

Johnsson, P.A., Eggleston, C.M., and Hochella, M.F., Jr. (1991) Imaging molecular-scale structure and microtopography of hematite with the atomic force microscope. American Mineralogist, 76, 1442–1445.

Kitano, Y., Okumura, M., and Idogaki, M. (1975) Incorporation of sodium, chloride and sulfate with calcium carbonate. Geochemical Journal, 9, 75–84.

——— (1979a) Influence of borate-boron on crystal form of calcium carbonate. Geochemical Journal, 13, 223–224.

——— (1979b) Behaviour of dissolved silica in parent solution at the formation of calcium carbonate. Geochemical Journal, 13, 253–260.

Meyer, G., and Amer, N.M. (1990) Optical-beam deflection atomic force microscopy: The NaCl (001) surface. Applied Physics Letters, 56, 2100–2101.

Mucci, A., and Morse, J.W. (1983) The incorporation of Mg^{2+} and Sr^{2+} into calcite overgrowths: Influences of growth rate and solution composition. Geochimica et Cosmochimica Acta, 47, 217–233.

——— (1985) Auger spectroscopy determination of the surface most adsorbed layer composition on aragonite, calcite, dolomite and magnesite in synthetic seawater. American Journal of Science, 285, 306–317.

Mucci, A., Morse, J.W., and Kaminsky, M.S. (1985) Auger spectroscopy analysis of magnesian calcite overgrowths precipitated from seawater and solutions of similar composition. American Journal of Science, 285, 289–305.

Reddy, M.M., and Wang, K.K. (1980) Crystallization of calcium carbonate in the presence of metal ions. Journal of Crystal Growth, 50, 470–480.

Reeder, R.J. (1983) Carbonates: Mineralogy and chemistry. Mineralogical Society of America Reviews in Mineralogy, 11, 394 p.

Reksten, K. (1990) Superstructures in calcite. American Mineralogist, 75, 807–812.

Söhnel, O., and Mullin, J. (1982) Precipitation of calcium carbonate. Journal of Crystal Growth, 60, 239–250.

Stipp, S.L., and Hochella, M.F., Jr. (1991) Structure and bonding environments at the calcite surface as observed with X-ray photoelectron spectroscopy (XPS) and low energy electron diffraction (LEED). Geochimica et Cosmochimica Acta, 55, 1723–1736.

Weisenhorn, A.L., Macdougall, J.E., Gould, S.A.C., Cox, S.D., Wise, W.S., Massie, J., Maivald, P., Elings, V.P., Stucky, G.D., and Hansma, P.K. (1990) Imaging and manipulating molecules on a zeolite surface with an atomic force microscope. Science, 247, 1330–1333.

Wicks, F.J., Kjoller, K., and Henderson, G.S. (1992) Imaging the hydroxyl surface of lizardite at atomic resolution with the atomic force microscope. Canadian Mineralogist, 30, 83–92.

Zachara, J.M., Kittrick, J.A., Dake, L.S., and Harsh, J.B. (1989) Solubility and surface spectroscopy of zinc precipitates on calcite. Geochimica et Cosmochimica Acta, 53, 9–19.

Manuscript received November 6, 1991
Manuscript accepted May 18, 1992